LHCD Current Profile Control Experiments towards Steady State Improved Confinement on JT-60U

S. Ide, O. Naito, T. Oikawa, T. Fujita, T. Kondoh, M. Seki, K. Ushigusa
and the JT-60 Team

Naka Fusion Research Establishment Japan Atomic Energy Research Institute
Naka-machi, Naka-gun, Ibaraki, 311-0193 Japan

Abstract

In JT-60U lower hybrid current drive (LHCD) experiments, a reversed magnetic shear configuration that was accompanied by the internal transport barriers was successfully maintained by means of LHCD almost in the full current drive quasi-steady state for 4.7 s. The normalized beta was kept near 1 and the neutron emission rate was almost steady as well indicating no accumulation of impurities into the plasma. Diagnostics data showed that all the profiles of the electron and ion temperatures, the electron density and the current profile were almost unchanged during the LHCD phase. Moreover, capability of LHCD in H-mode plasmas has been also investigated. It was found that the lower hybrid waves can be coupled to an H-mode edge plasma even with the plasma wall distance of about 14 cm. The maximum coupling distance was found to depend on the edge recycling.

1 Introduction

The lower hybrid wave (LHW) experiments on JT-60U has been oriented towards exploration of current drive and current profile control applicability for a steady state operation of a tokamak fusion reactor. Especially, confinement improvement and it's sustainment have been the most important issues. As recent experimental results in tokamak devices have shown [1–5], a reversed magnetic shear (R/S) plasmas with internal transport barriers (ITBs), in the temperatures and densities, are the most promising candidate for an advanced steady state operation of a tokamak fusion reactor. Towards that goal, it is important to investigate and demonstrate experimentally that a hollow current profile can be fully driven by the bootstrap current and external current driver(s) keeping the internal transport barriers accompanied. The lower hybrid current drive (LHCD) is the most suited scheme to investigate this scenario in present situation because of its high current drivability and profile controllability. On JT-60U, quasi-steady sustainment of a reversed magnetic shear configuration, control of the position of the internal transport barrier by shear control and formation of reversed magnetic shear by means of LHCD have been demonstrated in the previous experiments [6, 7]. However, in the reversed magnetic shear sustainment experiment, no clear internal transport barriers were not observed. Since then, sustainment of the internal transport barriers in a reversed magnetic shear plasma has been pursued. In this paper, results of the LHCD experiment for sustainment of the internal transport barriers in a reversed magnetic shear plasma is reported.

In a fusion reactor, plasmas will be expected to have an H-mode edge, because of not only better confinement but also for higher stability. However, it has been concerned if lower hybrid waves can be coupled to such plasmas and drive and control currents, since it is expected that in an H-mode edge plasma the electron density in the scrape off layer (SOL), outside the outermost closed flux surface, might be steeply decrease towards the LHW launchers. The experimental results of the wave coupling to H-mode edge plasmas are also presented in this paper.

2 Setup of experiments

The experiments were carried out with a single null divertor configuration, the major radius, R_0, and the minor radius, a, were about 3.6 m and 0.95 m, respectively. On the tokamak two multi-junction LHW

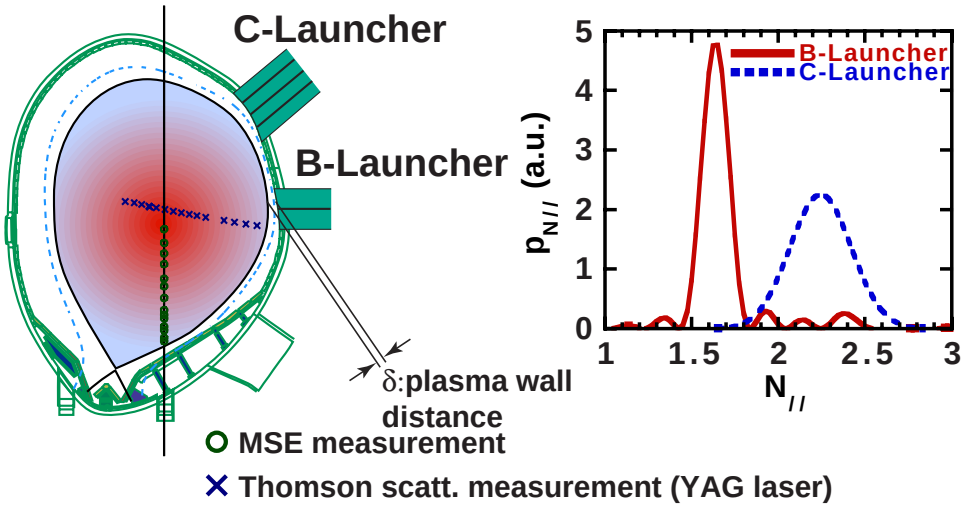

Figure 1: *Cross sectional view of a typical plasma which is discussed in this paper. The LHW "B-" and "C-" launchers are schematically shown. The power spectra of the waves injected from B-Launcher (solid line) and C-Launcher (dashed line) are also shown. They are normalized so as the integral is the same. The measuring positions of the MSE (open circles) and the YAG laser Thomson scattering system (crosses) are indicated.*

launchers are installed. One which is installed in a port at poloidal angle $\theta \approx 45^\circ$, is consists of four rows of eight multi-junction modules (MJ) which have 3 sub-waveguides and referred to as "C-Launcher" [8]. The other one is installed in a horizontal port and consist of four rows of four MJ modules which have 12 sub-waveguides [9, 10]. However, the lower two rows of the launcher has been no more used since the end of 1997. The rest upper two rows are referred to as "B-Launcher" in this paper. These launchers are schematically shown in Fig. 1. The spectra of the wave ray refractive index parallel to the magnetic field line($N_{\|}$) which were used in the internal transport barrier sustainment experiment shown in this paper are also shown in the same figure. One of the key parameters in wave-plasma coupling conditions is a spatial distance between the outermost closed flux surface. Since we have concentrated on coupling of waves injected from "B-Launcher" in the H-mode coupling experiment described in this paper, the typical distance for "B-Launcher" (δ) is also shown in the figure.

One of the most important measurement in this paper is the current profile measurement. A spatial profile of the safety factor (q), or a current density, was evaluated from data of the Motional Stark Effect (MSE) diagnostics [11]. The spatial points of the MSE measurement are indicated in Fig. 1 with open circles. The another important one is electron temperature and density measurements by means of Thomson scattering diagnostics using a YAG laser system. The measuring points are on a vertical line as shown in Fig. 1. Another Thomson scattering system which uses Ruby laser has lower repetition rate but more measuring points shares the same line of the sight of the YAG system.

3 Experimental results

3.1 Sustainment of internal transport barriers in a reversed magnetic shear plasma by LHCD

Firstly, experimental results of the internal transport barriers sustainment in a reversed magnetic shear plasma is shown. In Fig. 2 (a)-(d) temporal evolutions of the plasma current ($I_{\rm P}$), the injection powers ($P_{\rm inj}$) of the LHW and the neutral beam injection (NBI), the one turn loop voltage at the plasma surface (V_ℓ^{surf}), the internal inductance ($\ell_{\rm i}$), the normalized beta ($\beta_{\rm N}$), the reflection coefficient of the injected LHW ($R_{\rm LH}$) and the intensity of D_α line (D_α) are plotted. In the experiment, the toroidal magnetic field at the current center ($R_{\rm j} \simeq 3.55$ m) ($B_{\rm T0}$) was about 2.0 T and the working gas was deuterium. As shown in the figure, relatively higher NBI heating power ($P_{\rm NB}$) was applied during $I_{\rm P}$ ramp-up phase to

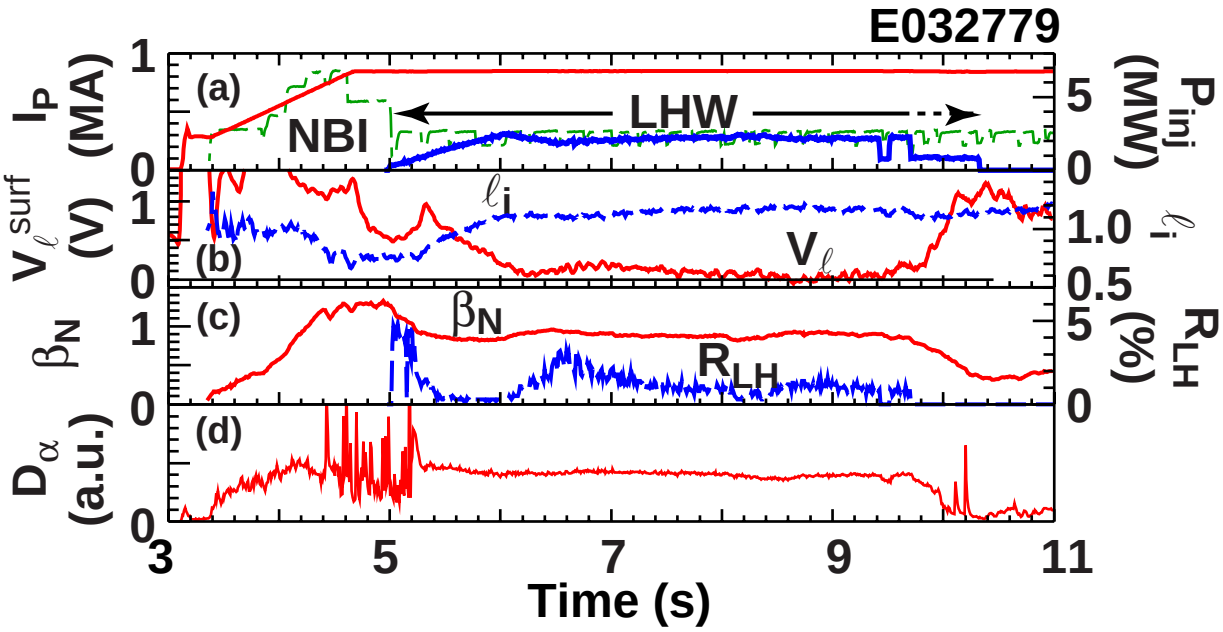

Figure 2: *Temporal evolutions of the plasma parameters, (a)* $I_{\rm P}$, $P_{\rm inj}$, *(b)* V_ℓ^{surf}, $\ell_{\rm i}$, *(c)* $\beta_{\rm N}$, $R_{\rm LH}$ *and (d)* D_α *of the plasma. The toroidal magnetic field at the current center was 2.0 T.*

form a reversed magnetic shear configuration by retarding the current penetration, and after $I_{\rm P}$ reached to the flat top $P_{\rm NB}$ was stepped down twice to the final value. The plasma has an H-mode edge until 5.2 s as indicated in the D_α emission signal (Fig. 1 (d)). On the other hand, at 5 s the LHW power ($P_{\rm LH}$) was turned on and $P_{\rm LH}$ was gradually increased up to around 2.5 MW ($\simeq$1.5 MW from B-Launcher and $\simeq$1 MW from C-Launcher) in 1 second. The $N_\parallel$ spectra of the injected waves from both launchers are shown in Fig. 1. The spectrum injected from C-Launcher was chosen so as the waves were to be absorbed in the outside the internal transport barrier and also to enhance the absorption of the lower $N_\parallel$ waves injected from B-Launcher [6, 7, 12]. Relatively lower $B_{\rm T}$ was chosen because of the following reasons: The plasma current should be around 1 MA, since we intended a full non-inductive current drive sustainment with limited $P_{\rm LH}$. Moreover, the effective safety factor ($q_{\rm eff}$) was also intended to be as low as around 5.5, so as to be comparable to the higher performance but NBI only cases. Therefore the value of $B_{\rm T0}$ was chosen to be 2.0 T. At this lower field, so called accessibility condition of the LHW can be significant especially in such a reversed magnetic shear plasma accompanied by the internal transport barriers in which $n_{\rm e}$ can be higher. The $N_\parallel$ spectrum of B-Launcher was then chosen so that the waves were to be blocked by the accessibility condition at the steep density gradient and would drive a hollow current profile more effectively. As $P_{\rm LH}$ increased, V_ℓ^{surf} decreased to zero and was kept almost constant during the application of the LHW as shown in the figure. The normalize beta ($\beta_{\rm N}$) was kept nearly constant as well. Around 7 s, $P_{\rm LH}$ decreased and V_ℓ^{surf} increased slightly. These should be attributed to an increase in $R_{\rm LH}$ as shown in Fig. 2 (c). This increase was caused simply by a fact that δ increased by about 2 cm. Since we directly controlled the position of the plasma center instead of δ, δ increased temporarily. However once δ came back to a small enough value V_ℓ^{surf} approached to zero, and even lower at around 8.5 s. B-Launcher stopped feeding power at around 9.7 s, and as soon as $P_{\rm LH}$ dropped $\beta_{\rm N}$ started decreasing and V_ℓ^{surf} jumped up. Although $\beta_{\rm N}$ seems to start decreasing even before the power drop, it is attributed to a short clamp in the B-Launcher injection at 9.4 s. Signals such as $\beta_{\rm N}$ decreased a little bit at the power clamp, they recovered as the power came back. It should be noted here that the neutron yield was kept constant as well indicating that no accumulation of impurity occurred. The confinement enhancement factor (H factor), based on the ITER-89 power law, should be of interest. Including all the injected power, $P_{\rm LH}$ and $P_{\rm NB}$, H was nominally estimated to be 1.2 at 9.1 s. However in the plasma configuration used here, as shown in Fig. 1, loss of high energy ions due to ripple in the toroidal magnetic field would not be negligible. Results of the orbit following Monte Carlo (OFMC)

code [13] indicated that the power lost via the ripple loss could be in excess of 30% of $P_{\rm NB}$. Suppose that the power lost via the ripple loss does not contribute at all, and so do not the shine through power and the lost power via charge exchange evaluated by the code, H can be as high as 1.4.

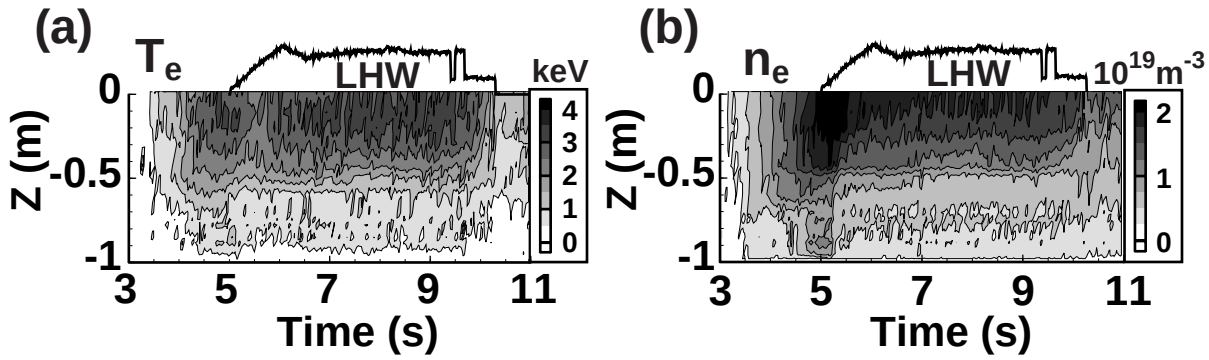

Figure 3: *Contour plots of the electron temperature (a) and density (b) measured by the YAG Thomson scattering system. The vertical axis (Z) corresponds to the vertical position of the measurement (cf. Fig. 1). A region where contour lines concentrate densely indicates the location of the internal transport barrier. It is almost unchanged in both profiles and at around $Z \simeq 0.5$ m. Moreover, it can be observed that internal transport barriers quickly disappears after $P_{\rm LH}$ dropped.*

Behavior of the internal transport barriers in the electron system during LHCD were well measured by the YAG Thomson scattering system. In Fig. 3, contour plots of the electron temperature $T_{\rm e}$ and the electron density $n_{\rm e}$ profile evolution are plotted. Here, Z referred to the vertical axis (c.f. Fig. 1), and the plasma current center located at around $Z \sim 0.2$ m. A steep increase in both $T_{\rm e}$ and $n_{\rm e}$ profiles, it would be recognized by a higher density of contour lines, at around $Z \simeq$ -0.6 – -0.5 m indicates existence of internal transport barriers. During the LHW injection the location of the internal transport barriers stays almost steadily. Immediately after P_{LH} faults at 9.7 s, the internal transport barriers shrink. This again implies the important role of LHCD.

Profiles of $T_{\rm e}$, $T_{\rm i}$ and $n_{\rm e}$ at 9.1 s, the very late phase of the LHCD, are shown in Fig. 4 (a) and (b) respectively. In all the profiles the gradient of a profile changes steeply at around $\rho \simeq 0.7$. However, the position of the shoulder, where a profile becomes flat towards the plasma center, looks different between $T_{\rm e}$ and $n_{\rm e}$ (the shoulder position is obscure in the $T_{\rm i}$ profile because of the limited line of the sight). The

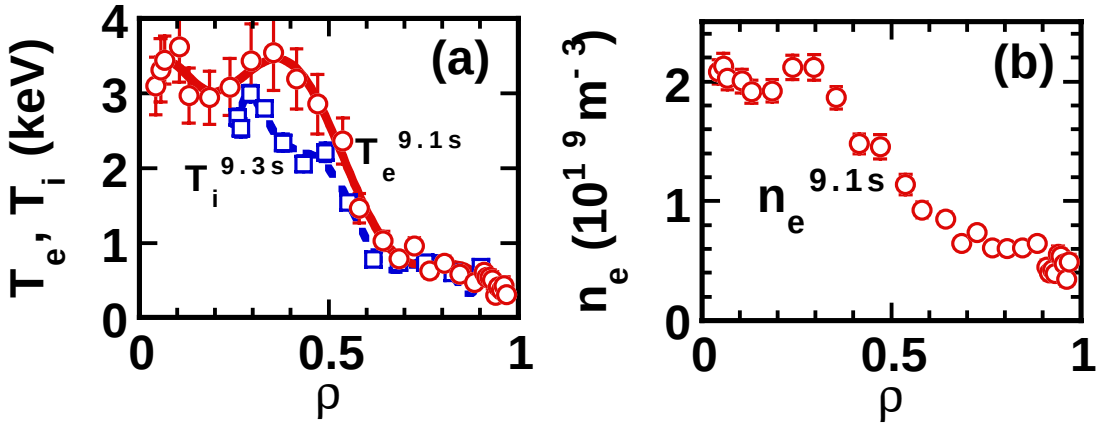

Figure 4: *The spatial profiles of the electron and ion temperatures (a) and the electron density (b). Both the electron temperature and density profiles were measured by the Ruby Thomson scattering system which shared the same line of sight as the YAG system used and more measurement points.*

gradient at the internal transport barrier in $T_{\rm e}$ profile seems to be much steeper than that in $n_{\rm e}$ profile. The electron temperature is higher than the ion temperature. The OFMC code can also provide how the NBI power was shared by the electrons and the ions. Evaluated fractional powers are 0.5 MW to the

electrons and 0.7 MW to the ions, respectively. Therefore the total power fed to the electrons is evaluated as 2.8 MW assuming that all the injected LHW power was absorbed by the electrons, while that to the ions is evaluated as 0.7 MW. This would be a cause of the higher temperature in the electrons than in the ions as shown in Fig. 4. However for further investigation such as a transport study, the power deposition profile of the LHW, which has not been obtained yet, should be required. Therefore it is not clear if electron heating was really dominant in the central region or not. The milder gradient in the electron density might be attributed to smaller beam fueling. It should be emphasized here that these situations are what would be expected in a fusion reactor.

Similarly in the current profile, it was found that the profile had been almost unchanged while V_ℓ^{surf} reached to nearly zero. Safety factor profiles are evaluated from the MSE measurement, and those at 4.9, 6.5, 7.5 and 9.1 s are plotted in Fig. 5 (a). It should be noted here that although the MSE diagnostics has

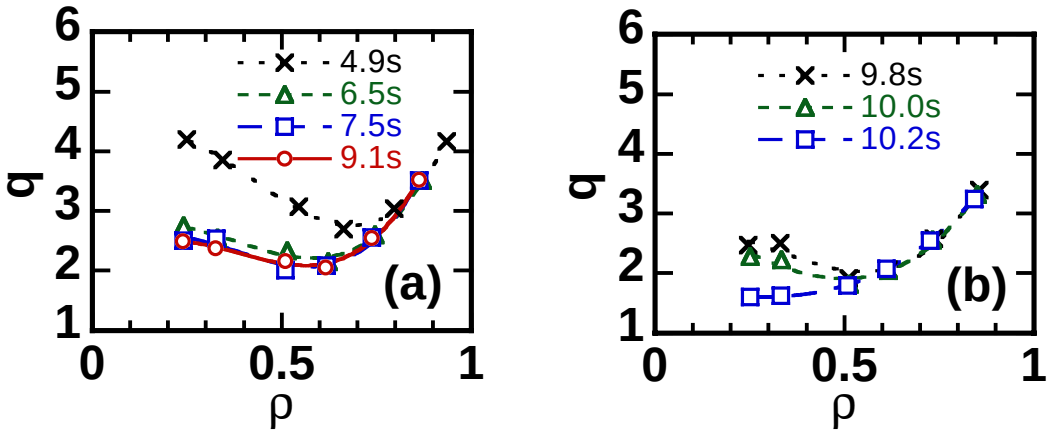

Figure 5: *The safety factor profiles evaluated from the MSE measurement before LHCD (4.9 s) and during LHCD (6.5, 7.5 and 9.1 s) (a). Also the decay of the q profile after $P_{\rm LH}$ dropped (9.8, 10.0, 10.2 s) is shown (b).*

nineteen measuring points, seven out of nineteen point data were used for the analysis. Mainly because that in this plasma configuration the pass length of the NBI beam which was used for the MSE measurement was relatively longer thus attenuation of the beam across the plasma center could be significant. As shown in the figure the profiles during the LHCD phase are very similar. However it should be noted here that the q profile at 7.5 s is slightly different from the other two. That is, the minimum value of q ($q_{\rm min}$) is slightly lower and the position of $q_{\rm min}$ seems to locate at about $\rho \simeq 0.5$, while at 6.5 s and 9.1 s it is about 0.5. This change should be attributed to the decrease of $P_{\rm LH}$ in the earlier phase (Fig. 2 (a)) that was mentioned before. Because of the reduction of the driving power, the driven current was expected to decrease. This would allow reorganization of the q profile. By taking a close look on Fig. 3, one can notice that the position of the internal transport barriers moved upward, i.e. toward the plasma center especially $n_{\rm e}$, corresponding to the change in the power (or more clearly in $R_{\rm LH}$ in Fig. 2 (c)). Again this fact emphasizes the importance of LHCD on the q control, and suggests possibility of active control of the location of the internal transport barriers. On the other hand in Fig. 5 (b), the decay of the q profile after $P_{\rm LH}$ dropped is shown for 9.8, 10.0 and 10.5 s. It is found that the negative magnetic shear was maintained until $P_{\rm LH}$ dropped and then it quickly disappeared.

In the later LHCD phase when V_ℓ^{surf} reached to zero, it was found that the polarization angle of MSE ($\gamma_{\rm MSE}$) reached almost constant in time at all the measured points. This means that V_ℓ was constant in radial direction and zero, since V_ℓ^{surf} was zero. Although the non-inductive portion of the plasma current can be evaluated even in cases where $V_\ell\ (\rho)\ \neq 0$ [14], this particular situation makes the evaluation of the driven current density profile by LHCD ($j_{LH}(\rho)$) very simple, since the inductive current density $j_{OH}(\rho)$ can be neglected. In this case the total current is expected to be consisted of the bootstrap current (j_{BS}), the beam driven current (j_{BD}) and j_{LH}. The first two components can be calculated easily by the ACCOME code [15]. The result shows that j_{BD} is negligibly small as expected, since the two tangential beams were in opposite directions thus balanced. Therefore j_{LH} can be evaluated by substituting j_{BS}

which is evaluated by the ACCOME code from the current profile measured in the MSE measurement. In Fig. 6, j_{tot}, j_{BS} and j_{LH} at 9.1 s are plotted. Since $T_{\rm i}$ profile was not available in the central region, the

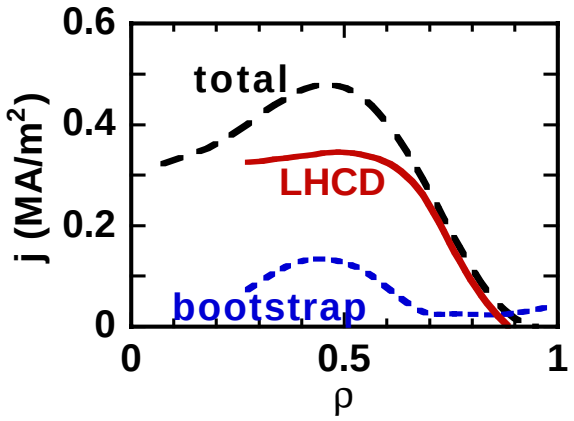

Figure 6: *The components of the total current (broken line). Since $V_\ell = 0$ can be assumed inside the plasma, $j_{\rm OH}$ can be neglected. The beam driven current was calculated and was very small as expected since the two tangential beams used were balanced. Therefore the dominating component of the current is the bootstrap current (dashed line) which is about 23% of the total current and the LH driven current (solid line).*

currents in the central region is not shown. It should be noted that although $T_{\rm i}$ profile was extrapolated towards the center to evaluate j_{BS} fraction, contribution from that area is not large due to smaller cross section. It is found that j_{LH} contributes mainly to sustain the hollow current profile. However, it is also found that j_{LH} does not seem to be small even inside the internal transport barriers where only higher $N_{\|}$ waves could access. Since the current driven by those higher $N_{\|}$ waves are small and the fractional injected power of those waves was relatively smaller, we firstly expected smaller $j_{\rm LH}$ inside the internal transport barriers. Detailed investigation should be required both in the analysis of the data and future experiments for this point. The amount of the bootstrap current is evaluated to be about 23% to the total current, therefore about 77% of the current is expected to be driven by LHCD. The nominal value of the current drive figure of merit can be estimated as about $1.3 \times 10^{19}{\rm MA/MW \cdot m^{-2}}$.

It should be noted here that in another shot in which higher $P_{\rm NB}$ of ~ 1 MW was added, higher $\beta_{\rm N}$ of more than 1.2 and H factor (evaluated nominally) of about 1.5 was sustained for about 2 s during LHCD. The internal transport barriers disappeared suddenly. This would be attributed to miss-alignment of the current profile. If so, quasi-steady sustainment of the internal transport barriers at higher $\beta_{\rm N}$ would be realized by fine adjustment of the current by LHCD.

3.2 LHCD on ELMy H-mode plasmas

In this subsection, results of LHCD on plasmas with an H-mode edge are shown. A plasma which has an H-mode edge is considered as a standard operational plasma in the ITER (international thermonuclear experimental reactor). Furthermore, even in an advanced scenario, that is a reversed magnetic shear operation, an H-mode edge would be preferable from a view point of stability [16]. However, few LHCD experiments on H-mode plasmas have been carried out.

Also in this experiment, a target plasma was of $I_{\rm P}$ = 0.85 MA, $B_{\rm T0} \simeq 2.0$ T and the working gas was deuterium. In Fig. 7 plotted are $P_{\rm LH}$ from B-Launcher, $P_{\rm NB}$, D_α, $R_{\rm LH}$ for the waves injected from B-Launcher and δ. As shown in the figure, low reflection coefficient ($\leq$ 10%) was maintained during ELM activities up to around 8.2 s when δ exceeded a certain value. This value of $R_{\rm LH}$ is low enough for B-Launcher to operate.

In Fig. 8 (a), (b) and (c) shown are the emission intensity of D_α emission intensity for three different shots. In each cases, $P_{\rm NB} \simeq$ 8.2, 6.0 and 5.0 MW, $P_{\rm LH} \simeq$ 1.4, 1.6 and 1.8 MW respectively during the period shown in the figure. The corresponding nominal H factor was 1.1, 1.2 and 1.3 respectively. Again here it is stressed that the nominal H factor might be under estimated since the ripple loss of the fast ions

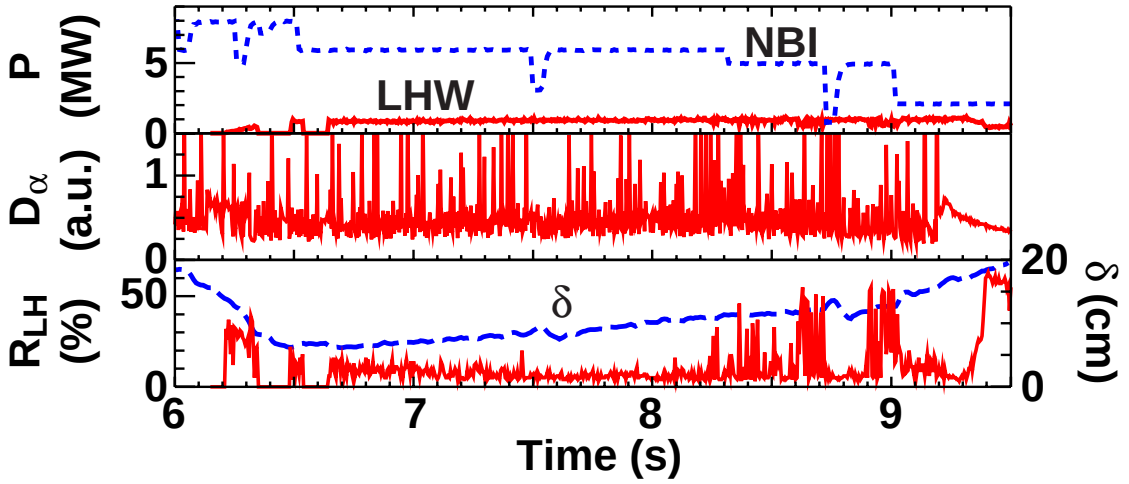

Figure 7: *(a) Temporal evolutions of $P_{\rm LH}$ from B-Launcher, $P_{\rm NB}$, D_α emission signal, $R_{\rm LH}$ for the waves injected from B-Launcher and the distance between the plasma and the first wall at the B-Launcher position. δ.*

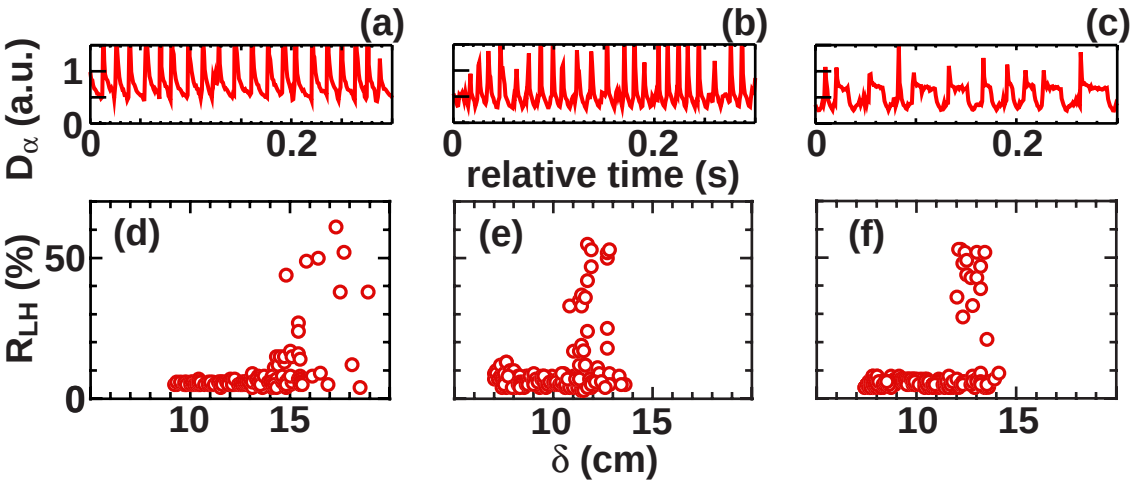

Figure 8: *(a) - (c) Temporal evolutions of D_α emission intensity. (d) - (f) Reflection coefficient for B-Launcher versus δ. $P_{\rm LH}$ from B-Launcher, $P_{\rm NB}$, D_α, $R_{\rm LH}$ and δ.*

is expected to be large in this configuration. Also in Fig. 8 (d), (e) and (f) shown are $R_{\rm LH}$ plotted against δ for each cases. As noted before, good coupling of low $R_{\rm LH}$ ($\leq \sim 10\%$) was found to be maintained up to a certain value of δ in the figure. In the case (a)/(d) the value reached to about 14 cm, while in the cases (b)/(e) it was about 11 cm. As is seen in the D_α signal, the baseline is different between the two cases and suggesting a difference in the edge recycling thus the SOL plasma condition. The higher D_α suggests higher SOL density which is preferable for LHW coupling. This is consistent with comparison between the two cases. On the other the case of (c)/(f) seems to come between the other cases. The base line of the D_α signal looks similar to that of the (b)/(e) case. However the activities of ELMs are different from the other two cases. The ELMs shown in Fig. 8 (c) are so called compound ELMs. A giant ELM triggers back transition from an H- to an L-mode, and the plasma stays at an L-mode for a while. Since an L-mode edge is expected to be preferable for better coupling, this compound ELMs might be the reason why $R_{\rm LH}$ in the case of (b)/(e) was better than that in the case of (b)/(e). Here, what should be emphasized here is on the LHCD feature. If a certain fraction of the current could not be driven appropriately, good coupling would be of small interest. In these case in fact, changes in the MSE signals were observed. For the discharge of the (b)/(e) case, the LH driven current was evaluated based on the MSE data. Different from the former experiment, $j_{\rm OH}$ should be taken into account since there left a certain V_ℓ in the plasma. The result showed that about 45% of the total current was driven

by the LHW. The current drive figure of merit can be estimated as about $1.0 \times 10^{19}\mathrm{MA/MW \cdot m^{-2}}$. The profile was off axis. This is as expected, however current profile controllability in H-mode plasmas should be investigated further.

4 Conclusions

On the JT-60U tokamak, quasi-steady sustainment of the internal transport barriers in a reversed magnetic shear configuration was demonstrated successfully in almost full non-inductive condition by means of LHCD. In the discharge, all the profiles of the electron and ion temperatures, the electron density and the current were found to be almost unchanged during LHCD. Moreover coupling of the LHW to H-mode plasmas were investigated and it was shown that LHW could be coupled even to H-mode edge plasmas up to the wall plasma separation of about 14 cm. The coupling seems to depend on the edge recycling, however further detailed study will be required for complete understanding. Substantial amount of LHCD was confirmed.

Acknowledgments

The authors would like to acknowledge all the members of Japan Atomic Energy Research Institute who have contributed to the JT-60U project.

References

[1] F. M. Levinton *et al.*, Phys. Rev. Lett. **75**, 4417 (1996).

[2] E. J. Strait *et al.*, Phys. Rev. Lett. **75**, 4421 (1996).

[3] X. Litaudon *et al.*, Plasma Phys. Controlled Fusion **38**, 1603 (1996).

[4] T. Fujita *et al.*, Phys. Rev. Lett. **78**, 2377 (1997).

[5] S. Ishida *et al.*, Phys. Rev. Lett. **79**, 3917 (1997).

[6] S. Ide, T. Fujita, O. Naito, and M. Seki, Plasma Phys. Controlled Fusion **38**, 1645 (1996).

[7] S. Ide *et al.,* in *the Sixteenth IAEA Fusion Energy Conference, Montréal, 1996* (IAEA, Vienna, 1997), Vol. 3, pp. 253–264.

[8] M. Seki *et al.*, in *the Sixteenth Symposium on Fusion Technology, London, 1990* (Elsevier Science Publishers, Amsterdam, 1991), Vol. 2, pp. 1060–1064.

[9] Y. Ikeda *et al.*, in *the Fourteenth Symposium on Fusion Engineering, San Diego, 1991* (IEEE, Piscataway, 1992), Vol. 1, pp. 122–125.

[10] Y. Ikeda *et al.*, Fusion Eng. Design **24**, 287 (1994).

[11] T. Fujita *et al.*, Fusion Eng. Design **34-35**, 289 (1996).

[12] S. Ide *et al.*, Phys. Rev. Lett. **73**, 2312 (1994).

[13] K. Tani, M. Azumi, H. Kishimoto, and S. Tamura, J. Phys. Soc. Japan **50**, 1726 (1981).

[14] T. Oikawa *et al.,* in *the seventeenth IAEA Fusion Energy Conference Yokohama, 1998* (IAEA, Vienna, 1998), pp. IAEA–F1–CN–69/CD1/1.

[15] K. Tani and M. Azumi, J. Comp. Phys **98**, 332 (1992).

[16] T. Fujita *et al.*, in *the seventeenth IAEA Fusion Energy Conference Yokohama, 1998* (IAEA, Vienna, 1998), pp. IAEA–F1–CN–69/EX1/2.